

# Hesperetin-Loaded Solid Lipid Nanoparticles and Nanostructure Lipid Carriers for Food Fortification: Preparation, Characterization, and Modeling

Milad Fathi · Jaleh Varshosaz · Mohebbat Mohebbi · Fakhri Shahidi

Received: 6 November 2011 / Accepted: 27 March 2012 / Published online: 5 May 2012  
© Springer Science+Business Media, LLC 2012

**Abstract** Solid lipid nanoparticles and nanostructure lipid carriers were used to entrap hesperetin and broaden confined knowledge of application of nanocarriers as the functional ingredients in food sectors. The produced nanocarriers using a high mechanical shear method were subjected to size and zeta potential analysis. The developed nanosize carriers had the encapsulation efficiency ranging from 39.90 to 63.08 %. Differential scanning calorimetry, X-ray diffraction, and Fourier transform infrared spectroscopy were also employed to study thermal behavior, crystalline state, and chemical structure. The release behavior of hesperetin in simulated gastrointestinal conditions was investigated and kinetically modeled. The modeling results indicated that the release phenomenon is mostly governed by combination of Fickian and dissolution mechanisms. Stability of the nanocarriers, as analyzed for up to 30 days, at 6 and 25 °C in aqueous suspension, showed no detectable hesperetin leakage. Cryoprotectant effect of different compounds (i.e., glucose, sorbitol, glycerin, lactose, and sucrose) was also examined. Finally, the potential capability of nanocarriers for food fortification was studied using milk as a model food. The fortified milk samples were subjected to sensory analysis and results betokened that the developed nanocarriers did not show any significant difference with blank milk sample and could well mask the bitter taste, after taste, and obviate poor solubility of hesperetin.

**Keywords** Hesperetin · Nanostructure lipid carriers · Solid lipid nanocarriers

## Introduction

Due to increase of public interest in healthier food, consumer demands have been toward functional foods. Encapsulation of bioactive food ingredients is a promising technique to protect them from environmental damage and mask their displeasure properties. Solid lipid nanoparticles (SLN) and nanostructure lipid carriers (NLC) are the new generations of nanovehicles and attracting increasing attention as the novel colloidal sensitive carriers in scientific and industrial applications (Pardeike et al. 2009). Compared with other encapsulation systems such as nanoemulsions and liposomes, SLN combine advantages such as providing better controlled release, slower degradation rate, and possibility of large scale production. In contrast to SLN that consist of solid lipid, NLC contain a certain amount of liquid lipid, which results in prevention of forming perfect crystals and expulsion phenomenon during storage (Fathi et al. 2012). SLN and NLC can both be produced applying biodegradable and biocompatible lipid without organic solvent, which make them very appropriate for food applications. Hentschel et al. (2008) used NLC for encapsulation of  $\beta$ -carotene using high-pressure melt-homogenization method. The produced nanocarriers showed emulsion stability, while a particle size of around 400 nm.

Hesperetin (5,7,3'-trihydroxy-4'-methoxy flavanone) belongs to flavonones which are abundantly found in citrus fruits (Tomás-Barberán and Clifford 2000). It is considered as a powerful antioxidant and has shown to inhibit chemically induced mammary tumorigenesis (So et al. 1996), colon carcinogenesis (Tanaka et al. 1997; Miyagi et al.

M. Fathi (✉) · M. Mohebbi · F. Shahidi  
Department of Food Science and Technology,  
Faculty of Agriculture, Ferdowsi University of Mashhad (FUM),  
Mashhad, Iran  
e-mail: milad.fathi@stu-mail.um.ac.ir

J. Varshosaz  
Department of Pharmaceutics, Faculty of Pharmacy,  
Isfahan University of Medical Sciences,  
Isfahan, Iran

2000), heart attack (Erlund 2004), and blood pressure (Borradaille et al. 1999; Horcajada and Coxam 2004). In spite of valuable benefits, its poor solubility in water (20 ppm or less) (Tommasini et al. 2005) and bitter taste impose considerable obstacles to food fortification. On the other hand, low solubility leads to a very low dissolution rate and bioavailability as well as an irregular absorption in the gastrointestinal tract (Sansone et al. 2009). The aims of the current study were to produce the novel nanoencapsulation systems (SLN and NLC), characterize, modulate their release profile, and investigate their potential application for food fortification.

## Materials and Methods

### Materials

Hesperetin was purchased from Sigma-Aldrich Company (Canada). Glycerol monostearate (GMS; Condea, Germany), stearic acid (SA; Merck, Germany), glyceryl behenate (Compritol® 888; Gattefossé, France), oleic acid (Sigma-Aldrich, Canada), and Tween 80 (Merck, Germany) were supplied at analytical grade. Estasan (caprylic/capric triglyceride) was kindly provided from BASF (The Chemical Company, Ludwigshafen, Germany). All other used chemicals and reagents were at least of analytical grade.

### Methods

#### SLN and NLC Production

In order to produce hesperetin-loaded SLN and NLC, aqueous and lipid phases were separately prepared. The total amount of lipid phase was kept constant (1 %) in all lipid nanocarriers. SLN contained solid lipid, while in NLC formulations, 15 % of the solid lipid was replaced by oil (Estasan and oleic acid). In this research, the effect of applied lipid (GMS and SA), hesperetin concentration (0.064 and 0.128 % (w/w) of emulsion), and kind of

nanocarrier (SLN and NLC) were studied. Due to formation of perfect crystals in the case of application of pure lipid, compritol was also added in all formulations. Table 1 provides the composition of all developed nanocarriers.

The aqueous phase at 80 °C was added to hesperetin containing melted lipid phase at the same temperature and stirred in 2,000 rpm for 1 min. The pre-emulsion was constructed by treatment using a bath sonication (Powersonic 505; Hwashin Technology, Gyeonggi-do, South Korea) for 15 min. The coarse emulsion was then subjected to probe sonication (Bandelin, Berlin, Germany) by TT13 probe for 1.5 min in amplitude and power of 50 % and 100 W, respectively. To prevent temperature increase, the probe sonicator was inactive in 2-s intervals. The attained emulsion was cooled down in an ice bath for 30 min to recrystallize lipid and form SLN or NLC. Subsequently, for future characterization, the nanocarrier dispersions were freeze-dried at -80 °C in 0.001 mbar for 48 h using a freeze dryer (Christ Alpha LD, Germany).

#### Encapsulation Load and Efficiency

Encapsulation efficiency (EE) and encapsulation load (EL) were determined using centrifugation method (Varshosaz et al. 2010a). A 1-ml SLN or NLC dispersion was placed in a Millipore tube with a cutoff of 10 kDa (Millipore, Bedford, MA, USA) and ultracentrifuged (Eppendorf, 5430; Germany) at 10,000 rpm for 10 min. The amount of free hesperetin in the filtrate phase was determined spectrophotometrically (Secomam, BP106, France) at wavelength of 276 nm. The encapsulation efficiency and encapsulation load were calculated based on the following equations:

$$EE = \frac{(W_T - W_F)}{W_T} \times 100 \quad (1)$$

$$EL = \frac{(W_T - W_F)}{(W_L)} \times 100 \quad (2)$$

where  $W_T$  is the total weight of applied hesperetin in

**Table 1** Formulation composition (percent weight/weight of emulsion) of solid lipid nanoparticles and nanostructure lipid carriers

Formulation code	Glycerol monostearate	Stearic acid	Compritol	Oleic acid	Estasan	Hesperetin
1	0.850	–	0.150	–	–	0.064
2	0.850	–	0.150	–	–	0.128
3	0.738	–	0.147	0.075	0.075	0.064
4	0.738	–	0.147	0.075	0.075	0.128
5	–	0.850	0.150	–	–	0.064
6	–	0.850	0.150	–	–	0.128
7	–	0.738	0.147	0.075	0.075	0.064
8	–	0.738	0.147	0.075	0.075	0.128

For all formulations, 2 % Tween 80 and up to 100 % purified water were added

formulation of nanocarrier,  $W_F$  is the amount of free hesperetin in filtrate phase, and  $W_L$  is the weight of the used lipid in preparation of the nanocarriers (Varshosaz et al. 2010b).

#### Particle Size and Zeta Potential

The average particle size and polydispersity index (PDI) of SLN and NLC were determined by photon electron spectroscopy using Zetasizer (NanoSizer 3000, Malvern Instruments, Malvern, UK) at the fixed angle of  $90^\circ$  using the volume distribution. The polydispersity index measures the size distribution of the nanocarriers. The lower the PDI, the narrower the size distribution. The zeta potential which is an indicator of surface charge was measured based on mean electrostatic mobility applying Helmholtz–Smoluchowski equation (Nash and Haeger 1966).

#### Morphology Characterization

Morphology of the nanocarriers was observed using transmission electron microscopy (TEM; LEO 912 ab, Zeiss Germany). Samples were negatively stained with uranyl acetate (2 %) and dried on carbon-coated grids at room temperature.

#### Hesperetin Release and Modeling

Hesperetin release was studied in gastric (pH of 1.2) and intestine (pH of 6.8) solutions applying dialysis bag method at  $37^\circ\text{C}$  and 100 rpm (Yang and Washington 2006). Three milliliters of hesperetin-loaded nanocarrier solution was sealed into dialysis bag (Sigma, Canada) with a 12-kDa cutoff. The bag was then placed into 50 ml gastric buffer for 2 h. It was subsequently subjected to intestinal buffer (60 ml) for 6 h. At certain time intervals, the amount of released hesperetin was determined spectrophotometrically at wavelength of 276 nm. The hesperetin release data were kinetically evaluated by zero-order, first-order, Higuchi, and Rigter–Peppas models (Higuchi 1963; Li et al. 2009; Sezer et al. 2011) (Eqs. 3–6):

$$C = Kt \quad (3)$$

$$C = [1 - \exp(-Kt)] \times 100 \quad (4)$$

$$C = Kt^{0.5} \quad (5)$$

$$C = Kt^n \quad (6)$$

where  $C$  is hesperetin concentration (percent) at time  $t$ ,  $K$  is kinetic constant, and  $n$  is release exponent. The latest is used

to characterize different release mechanisms. Encapsulant release from cylindrical carriers, with  $0.45 \leq n$  is controlled by Fickian diffusion mechanism,  $n > 0.89$  is commanded for dissolution phenomenon, and  $0.45 < n < 0.89$  is governed by combination of two mechanisms (Chakraborty et al. 2011).

#### Stability Study

To investigate the stability of produced nanocarriers against hesperetin leakage, the lipid dispersions were stored in polyethylene microtubes at room ( $25 \pm 1^\circ\text{C}$ ) and refrigeration ( $6 \pm 2^\circ\text{C}$ ) temperatures for a period of 30 days. The samples were analyzed at appropriate time intervals (0, 4, 10, 20, and 30 days) for percentage of remaining hesperetin in nanoparticles.

#### Cryoprotectant Effect

The nanocarrier solutions were diluted (1:1 %, v/v) with different cryoprotectant solutions of glucose, sorbitol, glycerin, lactose, and sucrose (1.5 %, w/v); froze at  $-80^\circ\text{C}$ ; and freeze-dried using aforementioned conditions. The lyophilized samples were reconstituted with deionized water, and their size, PDI, and zeta potential were determined (Schwarz and Mehnert 1997).

#### Thermal Analysis

The pure materials, hesperetin-free nanocarriers, and hesperetin-loaded nanocarriers were applied for thermal assessments. Differential scanning calorimetry (DSC) was performed using Setaram DSC Instrument (131, Germany) to measure melting point. About 5-mg sample was placed in standard aluminum sample pans and analyzed under nitrogen purge (50 ml/min). A heating rate of  $10^\circ\text{C}/\text{min}$  was employed in the range of  $0$ – $270^\circ\text{C}$  (Ficarra et al. 2002).

#### X-ray Diffraction Analysis

The crystallographic structural analysis was carried out by X-ray diffractometer (D8ADVANCE, Bruker, Germany) applying  $\text{Cu K}\alpha$  ( $\lambda = 1.5406 \text{ \AA}$ ). The samples (hesperetin, GMS, SA, compritol, and hesperetin free as well as hesperetin-loaded nanocarriers) were scanned over a  $2\theta$  of  $3$ – $50^\circ$  at a scan rate of  $0.05^\circ/\text{s}$  (Luykx et al. 2008).

#### Fourier Transform Infrared Spectroscopy

The infrared spectra were scanned on a Fourier transform infrared (FTIR) spectrophotometer (WQF-510; Bomem, Canada), at  $4 \text{ cm}^{-1}$  resolution in frequency range between  $3,800$  and  $800 \text{ cm}^{-1}$  using KBr Pellet method with sample to KBr ratio of 1:100.

**Table 2** Particle size, PDI, zeta potential, encapsulation efficiency, and encapsulation load of developed nanocarriers

Formulation code	Particle size (nm)	Polydispersity index	Zeta potential (mV)	Encapsulation efficiency (%)	Encapsulation load (%)
1	68.54±1.84 <sup>D</sup>	0.11±0.02 <sup>E</sup>	-4.76±0.33 <sup>B</sup>	57.37±0.59 <sup>BC</sup>	3.82±0.06 <sup>DE</sup>
2	73.13±2.47 <sup>D</sup>	0.20±0.02 <sup>DE</sup>	-3.55±0.08 <sup>D</sup>	42.90±2.18 <sup>E</sup>	5.72±0.29 <sup>B</sup>
3	63.91±0.60 <sup>D</sup>	0.21±0.02 <sup>D</sup>	-5.42±0.34 <sup>A</sup>	63.08±0.01 <sup>A</sup>	4.20±0.00 <sup>C</sup>
4	70.14±2.43 <sup>D</sup>	0.29±0.01 <sup>CD</sup>	-3.92±0.45 <sup>CD</sup>	43.87±1.31 <sup>DE</sup>	5.84±0.17 <sup>B</sup>
5	160.40±2.67 <sup>B</sup>	0.38±0.03 <sup>BC</sup>	-4.13±0.32 <sup>C</sup>	44.55±0.13 <sup>D</sup>	3.00±0.04 <sup>E</sup>
6	218.73±24.27 <sup>A</sup>	0.57±0.15 <sup>A</sup>	-3.04±0.46 <sup>E</sup>	39.90±0.87 <sup>F</sup>	5.31±0.17 <sup>BC</sup>
7	98.82±3.87 <sup>C</sup>	0.28±0.01 <sup>CD</sup>	-3.84±0.12 <sup>CD</sup>	59.84±5.18 <sup>AB</sup>	3.98±0.34 <sup>CD</sup>
8	173.77±8.66 <sup>B</sup>	0.41±0.02 <sup>B</sup>	-2.87±0.04 <sup>E</sup>	47.07±0.01 <sup>C</sup>	6.28±0.00 <sup>A</sup>

Values in each column followed by different letters are significantly different ( $p < 0.05$ )

### Sensory Properties

Milk was selected as a sample food system to study the potential application of produced nanocarriers for food fortification. Sensory evaluation of fortified milk samples was carried out using both oral and non-oral attributes by eight assessors who had much experience with sensory evaluation. Three milk samples, i.e., blank (2.5 % fat sterilized milk; Razavi Company), hesperetin-loaded nanocarrier fortified milk (0.1 %, w/v), and direct hesperetin fortified milk (at the same concentration contained in nanocarriers), were presented at temperature about 7 °C and assessed using hedonic scale of 1–7. Different sensory parameters were used for the descriptive analysis of milk samples including taste (creaminess, sweetness, bitter tastes after taste), color (yellowness), homogeneity, and total acceptance (Frost et al. 2001). The thickness of samples as a rheological parameter was also investigated, while no statistical difference was observed between three milk samples.

### Statistical Analysis

All experiments were performed at least with three replications, and average values were reported. Statistical analyses were carried out using MSTAT software (version C). Data were subjected to analysis of variance, and means were compared using “Duncan” test at 5 % significant level.

## Results and Discussion

### Particle Size, Zeta Potential, Encapsulation Efficiency, and Encapsulation Load

Hesperetin-loaded solid lipid nanoparticles and nanostructure lipid carriers were produced using high shear method, based on kind of applied lipid (GMS and SA), hesperetin concentration (0.064 and 0.128 % (w/w) of emulsion), and nature of nanocarriers (SLN and NLC). The mean values of

particle size (nanometers), PDI, zeta potential (millivolts), encapsulation efficiency (percent), and encapsulation load (percent) are tabulated in Table 2. The results showed that all produced nanocarriers (except formulation no. 6) had the PDI value lower than 0.5 indicating their narrow size distribution. The results revealed that GMS containing formulas had smaller size and narrower size distribution. On the other hand, NLC formulations showed smaller size in comparison to SLN formulations. It could be due to the less crystalline structure of NLC and therefore providing more space for hesperetin. Incorporating higher amount of hesperetin (0.128 % (w/w) of emulsion) in the developed nanocarriers led to significant ( $p < 0.05$ ) increase in nanoparticles' size. It may be attributed to the massive physical structure of hesperetin which occupied a huge volume of nanocarriers. Having the smaller size leads to higher stability against gravity due to Brownian motion of nanocarriers (Fathi et al. 2012). Zeta potential values of nanocarriers revealed that formulation no. 3 had the highest surface charge. The higher the zeta potential, the higher the repulsion force between nanoparticles and therefore the higher emulsion stability.

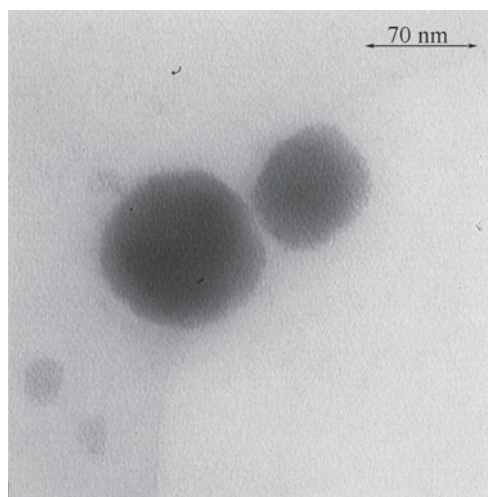


**Fig. 1** TEM morphology of formulation no. 3

Developed nanocarriers had encapsulation load ranging from 3.00 to 6.28 %. The higher the encapsulation load, the faster the release rate due to increase of driving force. By increasing encapsulation load, higher amount of encapsulant is targeted; however, encapsulation load more than 50 % leads to defect of carriers' surface (Acosta 2006). In the most cases, encapsulation efficiencies of SA containing nanocarriers were found to be lower than GMS formulations, which could be due to their crystalline structure (see "X-ray Diffraction Analysis" section). On the other hand, EE of all NLC formulations showed significantly ( $p < 0.05$ ) higher amount in comparison to SLN. The lipids of nanocarriers are recrystallized after cooling mostly in higher energy modifications, i.e.,  $\alpha$  and  $\beta'$  forms (Westesen et al. 1993). However, these configurations can transit into higher-order and lower-energy modification lattice,  $\beta$  form, which leads to have no room for guest molecules, encapsulant expulsion, and consequently decrease in encapsulation efficiency. This phenomenon is even more pronounced when pure lipids are used. Due to this reason, two different solid lipids (GMS or SA and compritol) were used in each formulation. Applying liquid lipid in the mixture led to

limitation of recrystallization and forming amorphous or less order crystalline state which resulted in imperfection and accommodation of higher amount for encapsulant.

Since all samples have similar images, formulation no. 3 was chosen as an example to study the morphology of nanocarrier using TEM (Fig. 1). The nanoparticles showed spherical and uniform shape.

### Hesperetin Release and Modeling

Figure 2 depicts the hesperetin release profiles of SLN and NLC. The release rate in first 2 h (gastric condition) appeared to follow the faster kinetics. It could be attributed to the faster dissolution of applied lipid in acidic condition or release of hesperetin from the surface of nanocarriers. Since the solubility of hesperetin in hot water (80 °C) is higher than cold water, after cooling the undissolved molecules start to adsorb on nanocarriers' surface. Nevertheless, the hesperetin release from formulation nos. 3 and 7 were found to be lower than 20 % at the first 2 h. The higher hesperetin-loaded nanocarriers showed the faster release profile, which is due to their higher driving force. On the

**Fig. 2** Release profile of hesperetin from different developed nanocarriers (formulation codes are based on Table 1)

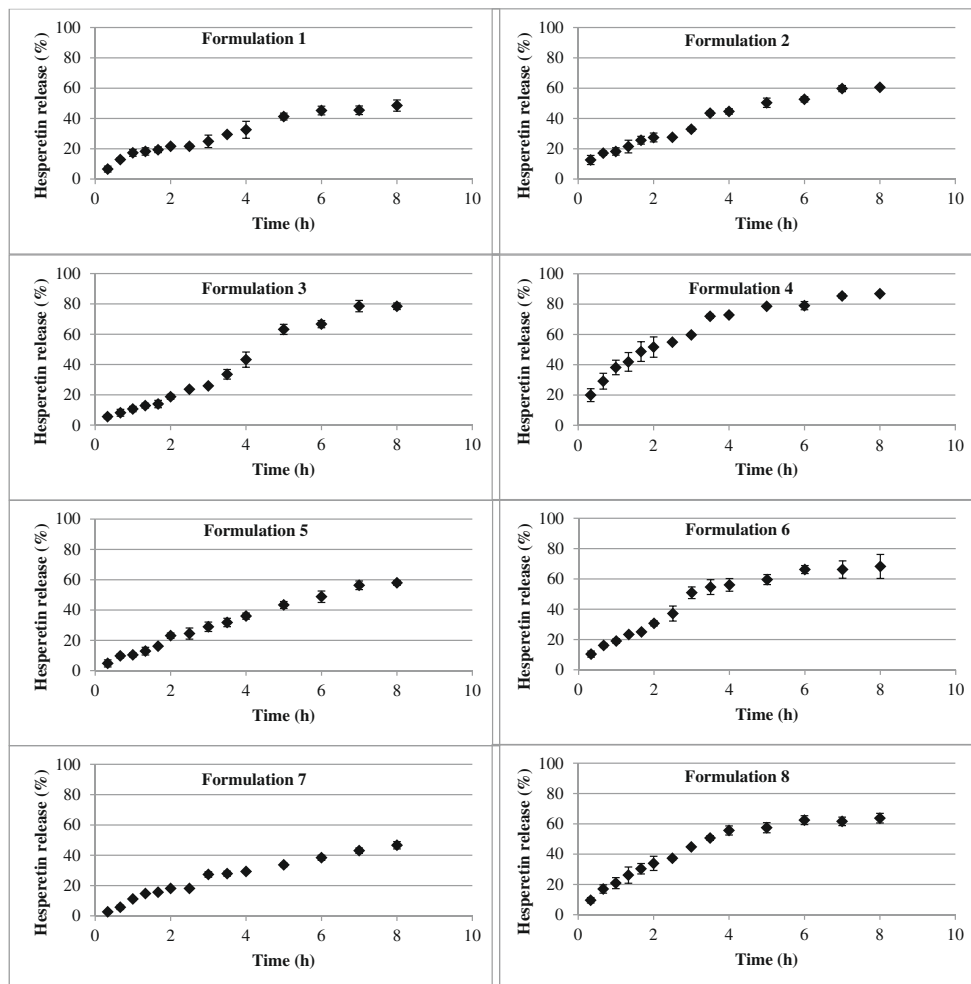




**Table 3** Model parameters of hesperetin release

Release condition	Formulation code	Zero order		Fist order		Higuchi		Rigter–Peppas		
		<i>K</i>	<i>R</i>	<i>K</i>	<i>R</i>	<i>K</i>	<i>R</i>	<i>K</i>	<i>n</i>	<i>R</i>
Gastric	1	12.6522	0.740	0.1430	0.882	15.4661	0.967	15.3026	0.5370	0.969
	2	15.8390	0.468	0.1853	0.651	19.4616	0.980	19.7211	0.4524	0.984
	3	9.0703	0.886	0.0985	0.913	10.9967	0.982	10.6240	0.6166	0.996
	4	30.1089	0.742	0.4210	0.961	36.8075	0.995	36.5591	0.5237	0.996
	5	10.7406	0.959	0.1178	0.958	12.7623	0.887	11.1759	0.9074	0.962
	6	16.5477	0.853	0.1942	0.901	20.1056	0.983	19.5893	0.5888	0.992
	7	9.6286	0.977	0.1047	0.981	11.3995	0.895	9.9638	0.9207	0.979
	8	18.6629	0.935	0.2236	0.973	22.5195	0.972	21.3427	0.6782	0.998
Intestinal	1	7.1073	0.860	0.0942	0.966	16.8711	0.945	12.8963	0.6612	0.973
	2	9.0510	0.736	0.1336	0.956	21.5911	0.955	18.5718	0.5849	0.964
	3	10.6672	0.968	0.1609	0.915	24.7582	0.840	10.3055	1.0194	0.968
	4	13.8763	0.752	0.3072	0.943	33.6128	0.870	42.8311	0.3527	0.952
	5	8.1370	0.945	0.1123	0.997	19.2140	0.943	12.7965	0.7431	0.995
	6	10.8726	0.903	0.1859	0.810	26.2683	0.899	31.2245	0.3952	0.930
	7	6.4996	0.879	0.8350	0.965	15.4159	0.951	11.5700	0.6711	0.981
	8	10.2551	0.733	0.1684	0.738	24.8006	0.893	30.0803	0.3829	0.935
Whole release process	1	7.3536	0.870	0.9887	0.945	16.6570	0.978	14.4730	0.5960	0.987
	2	9.3583	0.829	0.1403	0.947	21.3025	0.982	19.4289	0.5631	0.986
	3	10.5962	0.985	0.1522	0.954	22.6641	0.874	9.74860	1.0484	0.986
	4	14.5974	0.333	0.3442	0.958	34.0990	0.975	38.1523	0.4215	0.988
	5	8.2527	0.974	0.1129	0.997	18.2324	0.947	12.5300	0.7767	0.996
	6	11.1247	0.832	0.1874	0.973	25.3305	0.966	22.6032	0.5780	0.972
	7	6.6385	0.948	0.0854	0.983	14.8047	0.960	10.8763	0.7078	0.992
	8	10.6287	0.740	0.1774	0.948	24.4534	0.979	23.8719	0.5166	0.980

other hand, formulation no. 3 showed the better release profile, since lower burst release was observed in acidic condition and about 80 % of its encapsulant was released during the release time.

Hesperetin release from nanocarriers was kinetically studied using zero-order, first-order, Higuchi, and Rigter–Peppas models. Table 3 lists the model parameters and their corresponding correlation coefficients. For almost all of samples, based on their correlation coefficients, the best model was found to be Rigter–Peppas and the worst model was zero order. Lowest correlation coefficient for zero-order kinetic model indicated that hesperetin release from

nanocarriers is concentration dependent. The values of *n* for most of the nanocarriers were found to be  $0.45 < n < 0.89$ , betokened the release phenomenon is mainly governed by combination of both Fickian diffusion and dissolution mechanism. However, our results indicated that the nanocarriers did not show significant change ( $p > 0.05$ ) in their size during the release time.

Stability Analysis of Dispersion

About 1 ml of produced dispersion was kept in polyethylene microtubes for 30 days to study their stability against

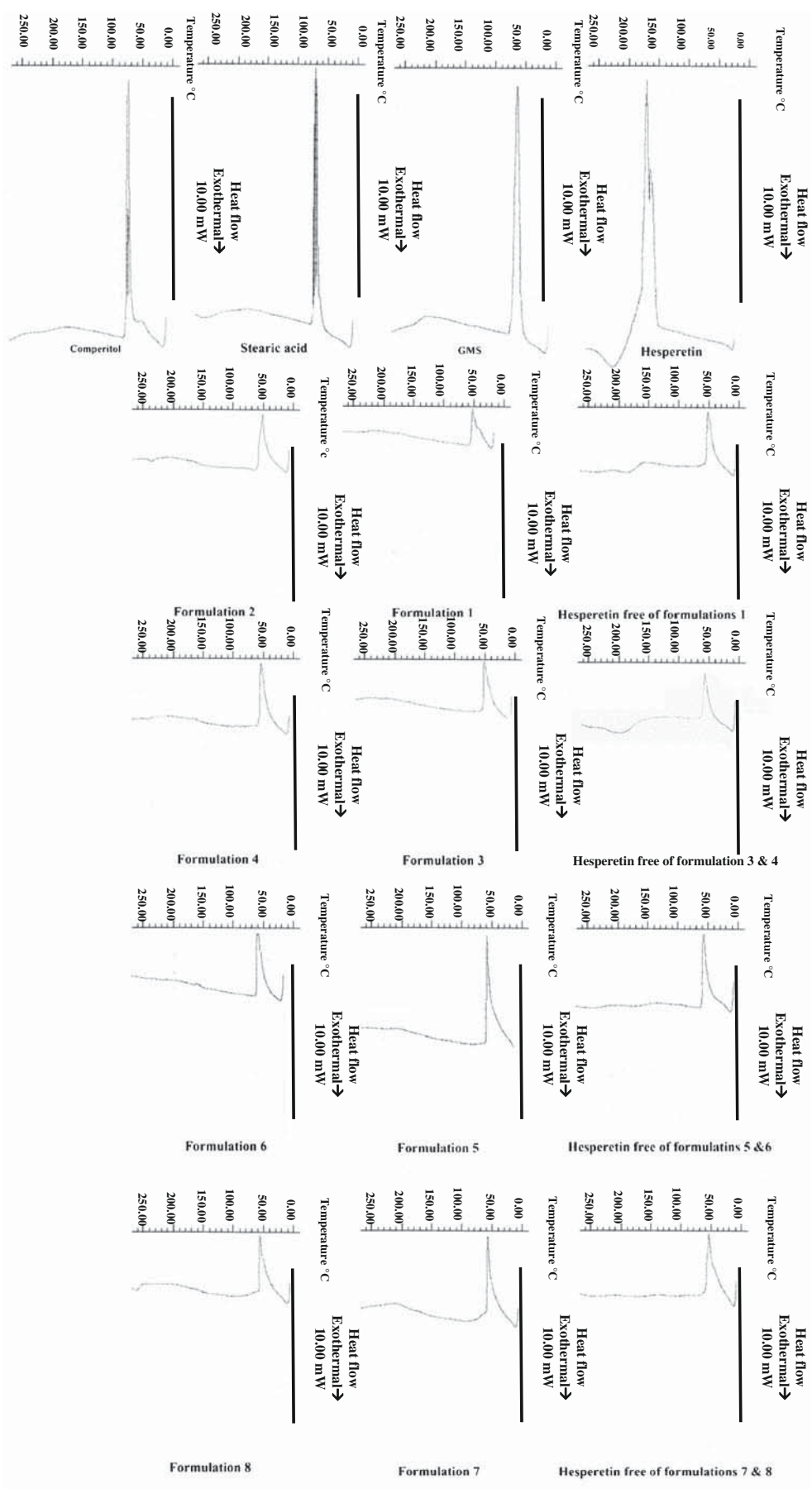
**Table 4** Cryoprotectant effect of different compounds on formulation no. 3

Cryoprotectant	Size (nm)	Polydispersity index (NS)	Zeta potential (mV)
Glucose	656.3±28.3A	0.36±0.03	-3.51±0.29B
Sorbitol	510.4±6.9B	0.28±0.01	-2.91±0.37C
Glycerin	598±17.9AB	0.32±0.02	-4.28±0.29A
Lactose	482.4±18.5C	0.28±0.01	-3.8±±0.20B
Sucrose	365.3±6.4D	0.27±0.01	-4.12±0.04A
Formulation no. 3	63.91±0.60	0.21±0.02	-5.42±0.34

Values in each column for cryoprotectant compound followed by different letters are significantly different ( $p < 0.05$ )

NS not significant

**Fig. 3** Thermograph of pure materials and different (based on Table 1) developed nanocarriers



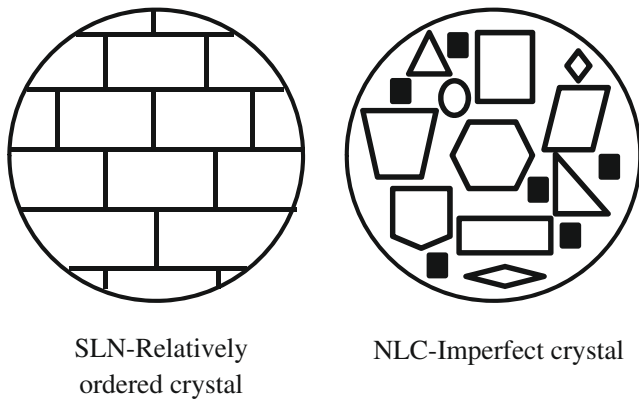


**Fig. 4** Relatively ordered crystal of SLN (*left*) imperfect crystal of NLC (*right*) (with permission from Müller et al. (2002))

hesperetin leakage. Size of nanocarriers showed a statistically significant ( $p < 0.05$ ) increase (micron size) while zeta potential did not change significantly ( $p > 0.05$ ). The increase of size of nanocarriers was due to their low zeta potential and high attraction force between particles which led to particle aggregation. A modification on production method or applied materials (e.g., application of mixtures of nonionic and ionic surfactants (Weiss et al. 2008)) may increase the surface charge and dispersion stability. On the other hand, the results indicated that the encapsulant leakage was not occurred, and the percentage of encapsulated hesperetin in nanocarriers did not changed more than 2 % (data not shown), which revealed that hesperetin is well incorporated into the lipid matrix.

Cryoprotectant Effect

The results of this study indicated that formulation no. 3 (NLC formulation containing GMS and 0.064 % hesperetin) had better properties in size, zeta potential, encapsulation efficiency, and hesperetin release; therefore, this sample was selected for analysis of cryoprotectant effect.

Particle aggregation during lyophilization could not be completely avoided. On the other hand, surface destruction occurred (Freitas and Muller 1998). Surface particle covering can protect the nanocarriers against the damage effect of shear forces. Carbohydrates and polyols have shown cryoprotecting effect for SLN and liposome suspensions (Crowe et al. 1986). Different cryoprotectants (i.e., glucose, sorbitol, glycerin, lactose, and sucrose) were applied, and the results of their size, PDI, and zeta potential after reconstruction were shown in Table 4. The best results were achieved with sucrose, which led to production of a fine powder and a solution with smallest size and lowest PDI after reconstruction. Some authors reported cryoprotectant concentrations up to 15 % for pharmaceutical applications (Schwarz and Mehnert 1997; Freitas and Muller 1998). However, our pretest showed that application of higher concentrations of cryoprotectant had a strong effect on sensory perceptions.

DSC Analysis

Thermal properties were assessed using DSC analysis to study melting point and crystallization status of the produced

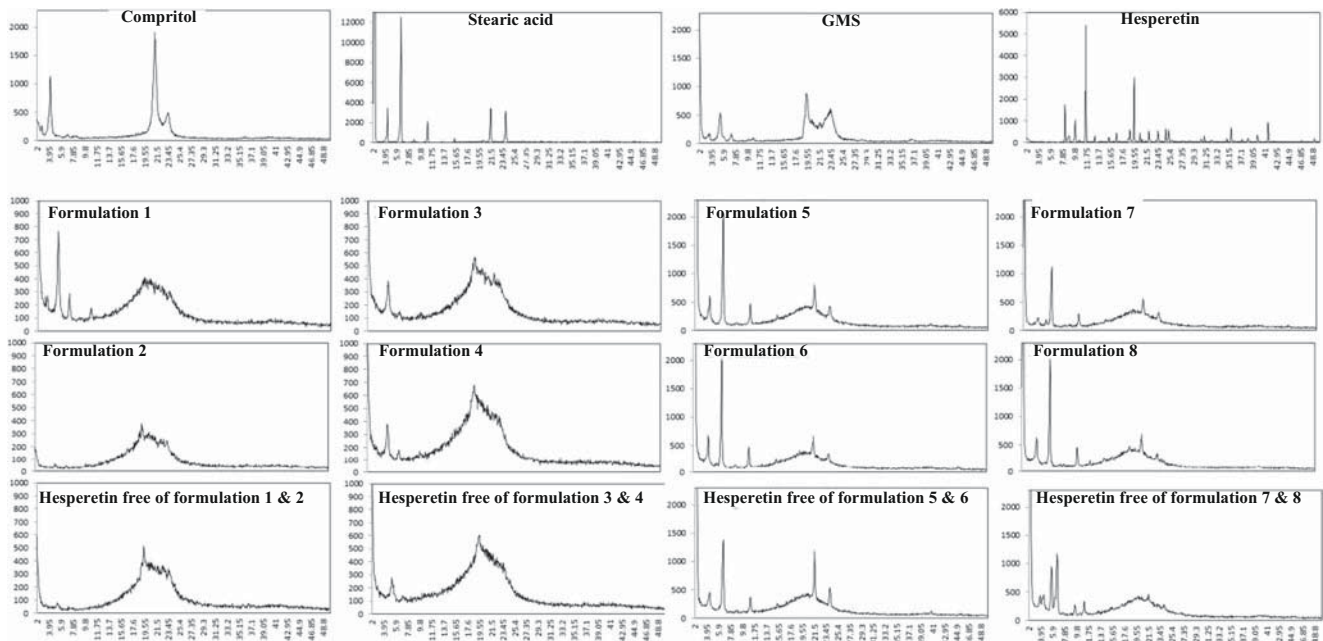


**Fig. 5** Diffractograms of pure materials and different (based on Table 1) developed nanocarriers



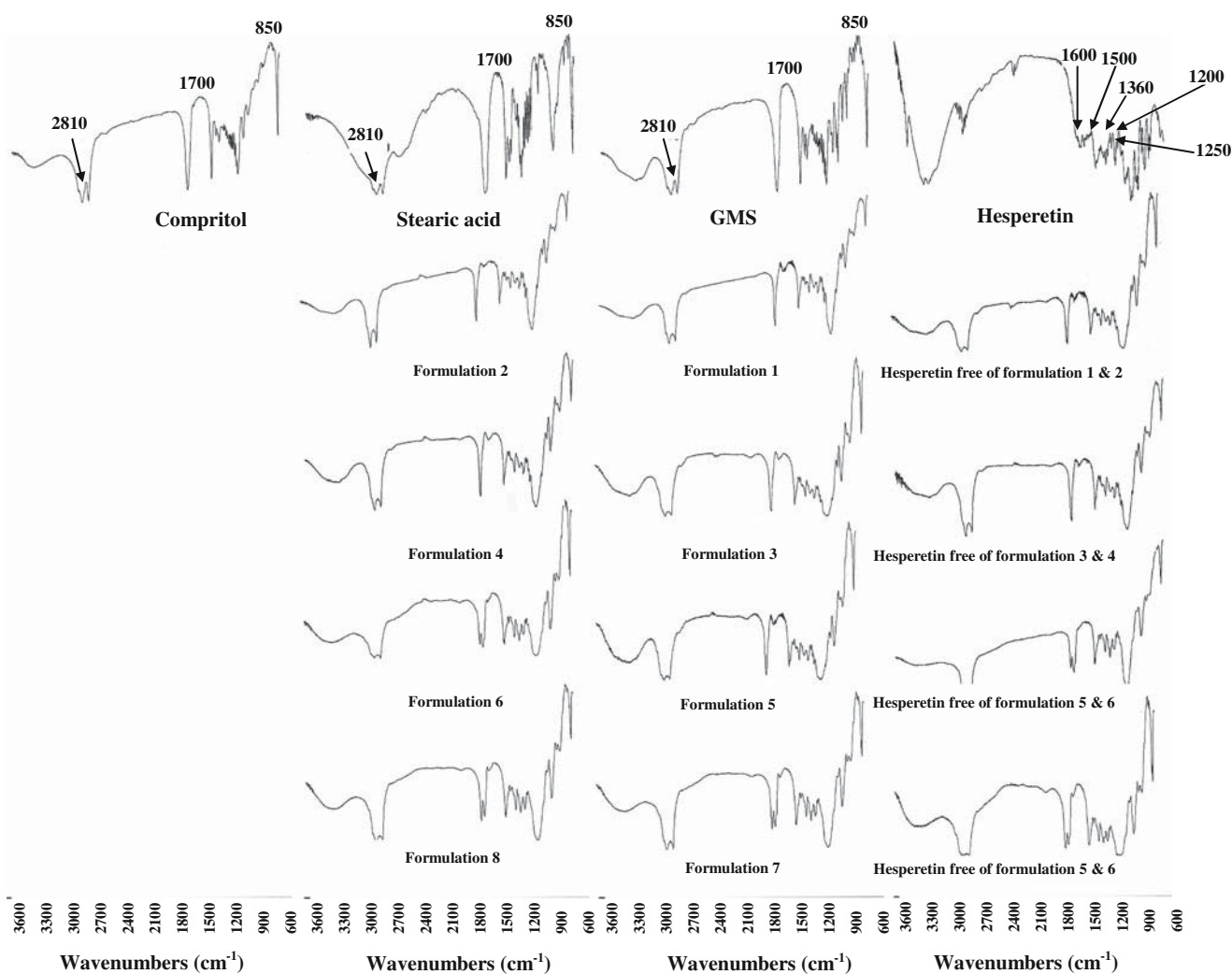


**Fig. 6** FTIR spectrum of pure materials and different (based on Table 1) developed nanocarriers

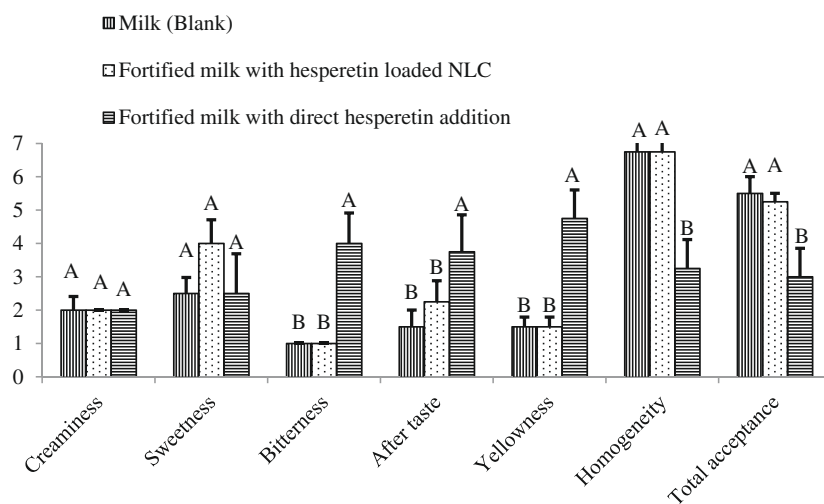
nanocarriers. Pure lipids and hesperetin showed large well-defined endotherm peaks indicating pure crystalline structure (Fig. 3). On the other hand, developed nanocarriers had shallow broad endothermic peaks showing their less ordered crystalline structure. It is due to application of different compounds with a range of molar mass that distorted the lattice structure (Gabbott 2008). It resulted in formation of a wide melting zone. However, all formulations showed a single peak, which approving that the pure compounds were well homogenized in developed matrices. Hesperetin showed a melting point at 165 °C. The thermograms of all developed hesperetin-loaded nanocarriers revealed no hesperetin peak around 165 °C, which representing that the encapsulant is properly incorporated into lipid carriers. All NLC formulations showed a statistically non-significant ( $p > 0.05$ ) melting point depression in comparison to SLN formulations due to dissolving of liquid lipid into solid lipid and producing a less ordered structure. As Fig. 4 shows, a less ordered crystal lipid matrix of NLC is favorable for entrapping more encapsulant

molecules in comparison to relatively ordered crystal of SLN. Melting points of SLN and NLC formulations were found to be significantly ( $p < 0.05$ ) lower than their corresponding bulk pure lipid. This suggests that the applied lipid might be in  $\beta'$  form in SLN and NLC (zur Muhlen et al. 1998). This melting point depression could be due to small particle size, high specific surface area, and the presence of surfactant. Similar tendency was also observed by Venkateswarlu and Manjunath (2004).

#### X-ray Diffraction Analysis

In order to identify the physical state of hesperetin-loaded nanocarriers, X-ray diffraction was performed. The diffractograms of pure compounds and unloaded as well as hesperetin-loaded SLN/NLC were presented in Fig. 5. The XRD pattern of pure hesperetin shows significant diffraction peaks at  $2\theta$  scattered angles of 8.3, 9.95, 11.7, 19.55, and 41.55, which informing its crystalline nature. The broad

**Fig. 7** Sensory results of fortified milk (different letters for each sensory feature indicating statistically significant differences;  $p < 0.05$ )



diffraction peaks of hesperetin-loaded nanocarriers indicate a reduction in crystallinity and  $\beta/\beta'$  form, which could be due to increase of impurity. This result was supported by thermograms obtained from DSC analysis in which a melting point depression is found compared to the pure materials. The peak intensity of NLC was less pronounced in comparison to SLN (at  $2\theta$  scattered angles of about 5.3 for GMS containing and 6.7 for SA containing nanocarriers) showing the less crystalline structure of NLC. The SA containing nanocarriers (formulation nos. 5 to 8) showed sharper peaks in contrast to GMS once, which revealed that these nanocarriers had the higher-order crystalline structure. Due to this reason, the encapsulation efficiency of SA was lower than GMS containing nanocarriers (Table 2).

#### FTIR Analysis

FTIR studies were conducted as a supplementary technique to find out any interaction between applied lipid and hesperetin to confirm the results obtained by the thermal analysis (Fig 6). Hesperetin revealed absorption bands of the aromatic multiple stretching from 1,500 to 1,600  $\text{cm}^{-1}$ , the –OH phenolic at 1,200 and 1,360  $\text{cm}^{-1}$ , and the methoxylic at 1,250  $\text{cm}^{-1}$ . Applied lipid (GMS, SA, and compritol) showed peaks corresponding to C=O stretching vibration (around 1,700  $\text{cm}^{-1}$ ) and OH–H bending vibration (850  $\text{cm}^{-1}$ ) of the hydrogen bond which are related to carboxylic acid group and also aliphatic C–H stretching (around 2,810  $\text{cm}^{-1}$ ). Spectrum comparison of pure encapsulant and developed nanocarriers showed that the aromatic bands of hesperetin and C=O band of applied lipids were overlaid but still recognizable, which revealed well entrapment of hesperetin in lipid matrix. On the other hand, no significant change of characteristics peaks (phenolic and methoxylic) of pure hesperetin spectra was observed in nanocarriers. This demonstrated that no chemical interaction

was occurred and hesperetin is compatible with applied lipids. These data supported the thermal results indicating that the absence of hesperetin peak in DSC diagram was due to well entrapment not the chemical reaction.

#### Sensory Analysis

In order to investigate the capability of developed nanocarriers for food fortification, the lyophilized nanocarriers were added to milk sample as a food system. Formulation no. 3 cryoprotected using sucrose, which showed the best characteristics, was selected for sensory analysis. The sensory results of blank, fortified with hesperetin-loaded nanocarriers and fortified milk using direct hesperetin addition, are depicted in Fig. 7. The allocated scores for hesperetin fortification indicated that direct hesperetin adding led to significant ( $p < 0.05$ ) increase in bitterness and yellowness and decrease in degree of homogeneity and total acceptance. Low homogeneity is due to low solubility of hesperetin in aqueous medium. On the other hand, surprising results were achieved from fortified milk using hesperetin-loaded nanocarriers, which no significant differences were obtained with blank milk sample in all studied sensory perceptions. Some of the advantages of nanoencapsulation are production of optically transparent carriers (due to having smaller size than visible wavelength), masking displeased flavor and increase emulsion stability. These results indicate that hesperetin cannot be directly added to milk sample and support the main idea of nanoencapsulation.

#### Conclusion

The aim of this paper was to assess the feasibility of lipid nanocarriers (SLN and NLC) for encapsulation of food bioactive ingredients. Hesperetin as a natural antioxidant

was loaded into SLN and NLC, and their characteristics were investigated. NLC samples showed the smaller size and higher encapsulation efficiency in comparison to SLN. Kinetic study in gastrointestinal conditions showed that the Rigter–Peppas is the best model for describing hesperetin release. Stability analysis indicated that the nanocarriers did not have any significant hesperetin leakage during 30 days storage. Sucrose was found to be the best cryoprotectant for nanocarrier lyophilization. DSC and XRD analyses showed that the crystalline states of produced nanocarriers were less ordered than pure materials and indicated that the hesperetin was well incorporated in lipid matrices. FTIR results revealed no chemical reaction between applied lipids and hesperetin. For the sake of analysis of capability of the developed encapsulation system in food sector, hesperetin-loaded nanocarriers were added to milk, and sensory perceptions of samples were investigated. Results showed that hesperetin cannot be directly added to milk and nanoencapsulation could improve the taste, homogeneity, and total acceptance. In spite of different advantages of developed nanocarriers, there were some obstacles that are mostly incorporated with lipid nanocarriers such as initial fast release and low surface charge, which should be overcome in future investigations.

**Acknowledgment** The authors would like to acknowledge the Iran National Science Foundation (INSF) for financial support under grant number of 89004288.

## References

- Acosta, E. (2006). Testing the effectiveness of nutrient delivery systems. In N. Garti (Ed.), *Delivery and controlled release of bioactives in foods and nutraceuticals*. Boca Raton: CRC.
- Borradaile, N., Carroll, K., & Kurowska, E. (1999). Regulation of HepG2 cell apolipoprotein B metabolism by the citrus flavanones hesperetin and naringenin. *Lipids*, 34(6), 591–598.
- Chakraborty, M., Dasgupta, S., Soundrapandian, C., Chakraborty, J., Ghosh, S., Mitra, M. K., & Basu, D. (2011). Methotrexate intercalated ZnAl-layered double hydroxide. *Journal of Solid State Chemistry*, 184(9), 2439–2445.
- Crowe, L. M., Womersley, C., Crowe, J. H., Reid, D., Appel, L., & Rudolph, A. (1986). Prevention of fusion and leakage in freeze-dried liposomes by carbohydrates. *Biochimica et Biophysica Acta (BBA) - Biomembranes*, 861, 131–140.
- Erlund, I. (2004). Review of the flavonoids quercetin, hesperetin, and naringenin. Dietary sources, bioactivities, bioavailability, and epidemiology. *Nutrition Research*, 24(10), 851–874.
- Fathi, M., Mozafari, M. R., & Mohebbi, M. (2012). Nanoencapsulation of food ingredients using lipid based delivery systems. *Trends in Food Science and Technology*, 23, 13–27.
- Ficarra, R., Tommasini, S., Raneri, D., Calabrò, M. L., Di Bella, M. R., Rustichelli, C., Gamberini, M. C., & Ficarra, P. (2002). Study of flavonoids/ $\beta$ -cyclodextrins inclusion complexes by NMR, FT-IR, DSC, X-ray investigation. *Journal of Pharmaceutical and Biomedical Analysis*, 29(6), 1005–1014.
- Freitas, C., & Muller, R. H. (1998). Spray-drying of solid lipid nanoparticles (SLNTM). *European Journal of Pharmaceutics and Biopharmaceutics*, 46(2), 145–151.
- Frost, M. B., Dijksterhuis, G., & Martens, M. (2001). Sensory perception of fat in milk. *Food Quality and Preference*, 12(5–7), 327–336.
- Gabbott, P. (2008). A practical introduction to differential scanning calorimetry. In P. Gabbott (Ed.), *Principles and applications of thermal analysis* (pp. 1–50). Oxford: Blackwell.
- Hentschel, A., Gramdorf, S., Müller, R. H., & Kurz, T. (2008).  $\beta$ -Carotene-loaded nanostructured lipid carriers. *Journal of Food Science*, 73(2), N1–N6.
- Higuchi, T. (1963). Mechanism of sustained-action medication: theoretical analysis of rate of release of solid drugs dispersed in solid matrices. *Journal of Pharmaceutical Sciences*, 52, 1145–1149.
- Horcajada, M. N., & Coxam, V. (2004). *Hesperidin, a citrus flavanone, improves bone acquisition and prevents skeletal impairment in rats in nutritional aspects of osteoporosis*. New York: Elsevier.
- Li, F., Jin, L., Han, J., Wei, M., & Li, C. (2009). Synthesis and controlled release properties of prednisone intercalated Mg–Al layered double hydroxide composite. *Industrial and Engineering Chemistry Research*, 48(12), 5590–5597.
- Luykx, D. M. A. M., Peters, R. J. B., van Ruth, S. M., & Bouwmeester, H. (2008). A review of analytical methods for the identification and characterization of nano delivery systems in food. *Journal of Agricultural and Food Chemistry*, 56(18), 8231–8247.
- Miyagi, Y., Om, A. S., Chee, K. M., & Bennink, M. R. (2000). Inhibition of azoxymethane-induced colon cancer by orange juice. *Nutrition and Cancer*, 36(2), 224–229.
- Müller, R. H., Radtke, M., & Wissing, S. A. (2002). Solid lipid nanoparticles (SLN) and nanostructured lipid carriers (NLC) in cosmetic and dermatological preparations. *Advanced Drug Delivery Reviews*, 54, S131–S155.
- Nash, R. A., & Haeger, B. E. (1966). Zeta potential in the development of pharmaceutical suspensions. *Journal of Pharmaceutical Sciences*, 55(8), 829–837.
- Pardeike, J., Hommoss, A., & Muller, R. H. (2009). Lipid nanoparticles (SLN, NLC) in cosmetic and pharmaceutical dermal products. *International Journal of Pharmaceutics*, 366(1–2), 170–184.
- Sansone, F., Rossi, A., Del Gaudio, P., De Simone, F., Aquino, R., & Lauro, M. (2009). Hesperidin gastroresistant microparticles by spray-drying: preparation, characterization, and dissolution profiles. *AAPS PharmSciTech*, 10(2), 391–401.
- Schwarz, C., & Mehnert, W. (1997). Freeze-drying of drug-free and drug-loaded solid lipid nanoparticles (SLN). *International Journal of Pharmaceutics*, 157(2), 171–179.
- Sezer, A. D., Kazak, H., Oner, E. T., & Akbuga, J. I. (2011). Levant-based nanocarrier system for peptide and protein drug delivery: optimization and influence of experimental parameters on the nanoparticle characteristics. *Carbohydrate Polymers*, 84(1), 358–363.
- So, F. V., Guthrie, N., Chambers, A. F., Moussa, M., & Carroll, K. K. (1996). Inhibition of human breast cancer cell proliferation and delay of mammary tumorigenesis by flavonoids and citrus juices. *Nutrition and Cancer*, 26(2), 167–181.
- Tanaka, T., Makita, H., Kawabata, K., Mori, H., Kakumoto, M., Satoh, K., Hara, A., Sumida, T., & Ogawa, H. (1997). Chemoprevention of azoxymethane-induced rat colon carcinogenesis by the naturally occurring flavonoids, diosmin and hesperidin. *Carcinogenesis*, 18(5), 957–965.
- Tomás-Barberán, F. A., & Clifford, M. N. (2000). Flavanones, chalcones and dihydrochalcones—nature, occurrence and dietary burden. *Journal of the Science of Food and Agriculture*, 80(7), 1073–1080.
- Tommasini, S., Calabrò, M. L., Stancanelli, R., Donato, P., Costa, C., Catania, S., Villari, V., Ficarra, P., & Ficarra, R. (2005). The inclusion complexes of hesperetin and its 7-rhamnoglucoside with

- (2-hydroxypropyl)-[beta]-cyclodextrin. *Journal of Pharmaceutical and Biomedical Analysis*, 39(3–4), 572–580.
- Varshosaz, J., Ghaffari, S., Khoshayand, M. R., Atyabi, F., Azami, S., & Kobarfard, F. (2010). Development and optimization of solid lipid nanoparticles of amikacin by central composite design. *Journal of Liposome Research*, 20(2), 97–104.
- Varshosaz, J., Minayian, M., & Moazen, E. (2010). Enhancement of oral bioavailability of pentoxifylline by solid lipid nanoparticles. *Journal of Liposome Research*, 20(2), 115–123.
- Venkateswarlu, V., & Manjunath, K. (2004). Preparation, characterization and in vitro release kinetics of clozapine solid lipid nanoparticles. *Journal of Controlled Release*, 95(3), 627–638.
- Weiss, J., Decker, E. A., McClements, D. J., Kristbergsson, K., Helgason, T., & Awad, T. (2008). Solid lipid nanoparticles as delivery systems for bioactive food components. *Food Biophysics*, 3, 146–154.
- Westesen, K., Siekmann, B., & Koch, M. H. J. (1993). Investigations on the physical state of lipid nanoparticles by synchrotron radiation X-ray diffraction. *International Journal of Pharmaceutical*, 93, 189–199.
- Yang, S., & Washington, C. (2006). Drug release from microparticulate systems. In S. Benita (Ed.), *Microencapsulation: methods and industrial applications*. New York: Taylor & Francis Group.
- zur Muhlen, A., Schwarz, C., & Mehnert, W. (1998). Solid lipid nanoparticles (SLN) for controlled drug delivery—drug release and release mechanism. *European Journal of Pharmaceutics and Biopharmaceutics*, 45(2), 149–155.